

# Journal of the European Ceramic Society

## The Effect of Airborne-particle Abrasion and Regeneration Firing on the Strength and Reliability of Translucent Zirconia Dental Ceramics

--Manuscript Draft--

<b>Manuscript Number:</b>	
<b>Article Type:</b>	Full Length Article
<b>Keywords:</b>	zirconia; dental ceramics; phase transformation; microstructure, Weibull statistics
<b>Corresponding Author:</b>	Andraž Kocjan Jozef Stefan Institute Ljubljana, SLOVENIA
<b>First Author:</b>	Tadej Mirt
<b>Order of Authors:</b>	Tadej Mirt Anže Abram Nigel Van de Velde Ivan Jerman Raul Bermejo Andraž Kocjan Peter Jevnikar
<b>Abstract:</b>	<p>Air-particle abrasion (APA) of zirconia dental ceramics is a universally accepted laboratory surface roughening procedure. APA may substantially increase strength of 3Y-TZP, which is associated with (sub)surface compressive residual stresses through t-m phase transformation. In this work, the effects of APA and regeneration firing (RF) (1000 °C, 15 min) of various zirconia dental ceramics, containing 3–5 mol.% of yttria, were investigated. The phase composition, (sub)surface microstructural changes and biaxial flexural strengths along with Weibull statistics and fractography were analysed and compared. The results show a significant increase in strength for 3Y and 4Y specimens after APA, ascribed to the t-m transformation toughening. However, APA substantially decreased the strength of 5Y variant. After RF, the ferroelastic domain switching phenomenon was presumably the persisting mechanism to withstand the propagation of APA-induced cracks in 3Y and 4Y zirconia materials, not being inferior to strength values of the as-sintered counterparts.</p>
<b>Suggested Reviewers:</b>	Fei Zhang fei.zhang@kuleuven.be  Laurent Gremillard laurent.gremillard@insa-lyon.fr  Susanne Scherrer susanne.scherrer@unige.ch

## Highlights

1. Airborne-particle abrasion (APA) increases the characteristic strength and reliability of the 3 and 4 mol.% yttria-stabilized dental zirconia ceramics.
2. Strength values of regeneration fired (RF) 3Y- and 4Y-zirconia specimens after APA were in agreement to strength values of the as-sintered counterparts.
3. RF reversed the APA-induced *t-m* phase transformation in 3Y- and 4Y-zirconia specimens, while the ferroelastic domain switching phenomenon persisted.
4. APA substantially decreased the strength and reliability of 5Y variant.

# The Effect of Airborne-particle Abrasion and Regeneration Firing on the Strength and Reliability of Translucent Zirconia Dental Ceramics

Tadej Mirt,<sup>a</sup> Anže Abram,<sup>b</sup> Nigel Van de Velde,<sup>c</sup> Ivan Jerman,<sup>c</sup> Raul Bermejo,<sup>d</sup> Andraž Kocjan,<sup>\*b</sup> Peter Jevnikar<sup>a</sup>

<sup>a</sup>Department of Prosthodontics, Faculty of Medicine, University of Ljubljana, Hrvatski trg 6, SI-1000 Ljubljana, Slovenia

<sup>b</sup>Department for Nanostructured Materials, Jožef Stefan Institute, Jamova 39, SI-1000 Ljubljana, Slovenia

<sup>c</sup>National Institute of Chemistry, Hajdrihova 19, SI-1000 Ljubljana, Slovenia

<sup>d</sup>Department of Materials Science, Montanuniversität Leoben, A-8700 Leoben, Austria

\*Corresponding author: [a.kocjan@ijs.si](mailto:a.kocjan@ijs.si)

## Abstract

Air-particle abrasion (APA) of zirconia dental ceramics is a universally accepted laboratory surface roughening procedure. APA may substantially increase strength of 3Y-TZP, which is associated with (sub)surface compressive residual stresses through *t-m* phase transformation. In this work, the effects of APA and regeneration firing (RF) (1000 °C, 15 min) of various zirconia dental ceramics, containing 3–5 mol.% of yttria, were investigated. The phase composition, (sub)surface microstructural changes and biaxial flexural strengths along with Weibull statistics and fractography were analysed and compared. The results show a significant increase in strength for 3Y and 4Y specimens after APA, ascribed to the *t-m* transformation toughening. However, APA substantially decreased the strength of 5Y variant. After RF, the ferroelastic domain switching phenomenon was presumably the persisting mechanism to withstand the propagation of APA-induced cracks in 3Y and 4Y zirconia materials, not being inferior to strength values of the as-sintered counterparts.

**Keywords:** zirconia; dental ceramics; phase transformation; microstructure, Weibull statistics

## 1. Introduction

1 Zirconia ceramic stabilized with 3 mol% yttria (3Y-TZP) is considered the first generation of  
2 zirconia used for dental ceramics. It possesses excellent room temperature mechanical  
3 properties associated with the *tetragonal-to-monoclinic* ( $t \rightarrow m$ ) transformation toughening  
4 mechanism [1]. However, the moisture-induced spontaneous  $t \rightarrow m$  transformation of zirconia  
5 in humid environments (known as low temperature degradation (LTD) or ageing) is said to  
6 contribute to the degradation of the material, starting at the surface, with the corresponding  
7 decrease in mechanical properties [2–4]. For dental applications, biocompatibility and  
8 aesthetics are also important factors in the use of zirconia ceramics. 3Y-TZP has successfully  
9 replaced metal frameworks in porcelain fused to the metal fixed dental prostheses (FDP).  
10 Recently, new generations of super- and ultra-translucent zirconia ceramics with superior  
11 aesthetic features have been successfully fabricated [5]. Their composition has been tailored  
12 by altering doping elements, for instance, increasing the amount of yttria ( $Y_2O_3$ ) to 4 or 5 mol.%  
13 and/or reducing the amount of alumina ( $Al_2O_3$ ) ( $\leq 0.1$  wt%). This has enabled the use of zirconia  
14 in a monolithic form, e. g., as single crowns, occlusal veneers, or frontal area FDPs, among  
15 others [6]. However, the relatively high content of yttria (i.e. 4 to 5 mol.%) leads to  
16 overstabilized tetragonal crystal lattice, which in turn restrain the  $t \rightarrow m$  toughening, with the  
17 corresponding detriment in material's strength [7–10]. On the other hand, it contributes to the  
18 maturation of a mechanically inferior and optically isotropic cubic crystal phase. This phase  
19 minimizes the scattering of the incident light, enhancing the translucency, but with a lower  
20 mechanical strength as a trade-off, leaving the material more susceptible to the progression of  
21 intrinsic and process-introduced flaws. The combination of aesthetics and still sufficient  
22 mechanical strength of translucent zirconia ceramics has encouraged the fabrication of thin,  
23 non-retentive restorations in the visible frontal area, i. e., the resin-bonded fixed dental  
24 prostheses [11], fulfilling the directions towards the concepts of minimally invasive dentistry. In  
25 this regard, the bonding of these restorations to tooth structures is decisively dependent on the  
26 adhesion of zirconia ceramic to resin cement. Besides the chemical promotion with 10-  
27 methacryloyloxydecyl dihydrogen phosphate (MDP-10) monomer, the zirconia-resin adhesion  
28 can be well enhanced mechanically with a low-pressure airborne-particle abrasion (APA) of  
29  
30  
31  
32  
33  
34  
35  
36  
37  
38  
39  
40  
41  
42  
43  
44  
45  
46  
47  
48  
49  
50  
51  
52  
53  
54  
55  
56  
57  
58  
59  
60  
61  
62  
63  
64  
65

1 the zirconia surface [12]. It has been shown that APA improves the mechanical properties of  
2 the 3Y-TZP [13] and the materials' ageing stability [14], presumably by introducing  
3 compressive residual stress at the materials' surface through the stress-induced  $t \rightarrow m$  phase  
4 transformation. Nevertheless, it has been speculated that APA might introduce subsurface  
5 cracks and flaws into the zirconia, hence weakening the material. When the strengthening  
6 potential of 3Y-TZP is partially or entirely abolished in new generations of zirconia, surface  
7 damaging procedures could have a detrimental effect on mechanical integrity [10,15].

13 Besides APA, the final shaping of dental restorations requires additional invasive modification  
14 processes, such as grinding, polishing, and diamond drilling, to achieve proper morphology  
15 and specific surface finish. Manufacturers of zirconia ceramics have recommended various  
16 surface treatments, including heat treatment, which can act as a type of regeneration firing, to  
17 re-establish the tetragonal crystal structure after shaping modifications, aiming to increase the  
18 reliability of the 3Y-TZP. When heat treatments are used, the reverse transformation,  $m \rightarrow t$ ,  
19 can occur, and the compressive stresses can be relieved, decreasing the flexural strength but  
20 regaining the stress-induced transformation toughening mechanism. Despite the decrease in  
21 strength, the material may become more stable and reliable [16–18]. When the heat treatment  
22 is employed for new generations of zirconia that contain less tetragonal phase, its effects  
23 should be negligible.

37 The compromising effects of APA on the structural integrity of novel translucent zirconia have  
38 recently been shown to make the material more prone to APA-induced crack propagation  
39 under applied stresses [10,15]. Moreover, evidence of the effects of heat treatment on the  
40 intrinsic properties of novel translucent zirconia ceramics is lacking in the literature. Therefore,  
41 the present study aims to evaluate and compare the effects of APA before and after heat  
42 treatment on the mechanical strength and reliability of the high-, super- and ultra-translucent  
43 zirconia ceramics, as compared to traditional (3Y-TZP) zirconia ceramics.

## 2. Materials and methods

### 2.1 Specimen preparation

1  
2  
3 Disk-shaped specimens were fabricated from four commercially available, ready-to-press,  
4 biomedical-grade zirconia powders TZ-3YB-E, TZ-PX-242A, Zpex4, and ZpexSmile (Tosoh,  
5 Tokyo, Japan). The content of yttria stabilizer in TZ-3YB-E and TZ-PX-242A is 3 mol.%, and 4  
6 and 5 mol.% in Zpex4 and ZpexSmile, respectively. The TZ-3YB-E powder contains 0.25 wt.%  
7 of alumina addition, whereas the percentage of alumina in TZ-PX-242A, Zpex4, and ZpexSmile  
8 is lower (0.05 wt.%). The powders are granulated and contain about 3 wt.% of inorganic binder,  
9 enabling dry pressing. These materials are commonly used in the fabrication of biscuit-sintered  
10 zirconia blanks for CAD/CAM machining. The resulting ceramic powders, TZ-3YB-E, TZ-PX-  
11 242A, Zpex4, and ZpexSmile, were referred to as 3Y, 3Y-T, 4Y, and 5Y throughout the text,  
12 respectively.  
13  
14  
15  
16  
17  
18  
19  
20  
21  
22  
23  
24  
25

26 The uniaxial dry pressing in a floating die, at 147 MPa with a dwell time of 30 s, was used to  
27 shape green discs, which were 20 mm in diameter and 2 mm thick (PW 10, P/O/Weber,  
28 Remshalden, Germany). According to the powder supplier recommendations, these discs  
29 were subsequently presintered at 1000°C for 1 h and subsequently pressure-less sintered in  
30 air at 1450°C for 2 h (Nabertherm GmbH, Lilienthal, Germany). After firing, each group of  
31 zirconia ceramic consisted of 120 disc-shaped specimens, yielding a total of 480 specimens  
32 for the characterization. The final diameters and thicknesses of specimen discs are presented  
33 in Table S1 (Supplementary Material). Relative density was measured according to  
34 Archimedes' method using deionized water as the immersion liquid. All materials reached  
35 approximate levels of theoretical density provided by the manufacturer (Table S1,  
36 Supplementary Material).  
37  
38  
39  
40  
41  
42  
43  
44  
45  
46  
47  
48  
49  
50  
51  
52  
53  
54  
55  
56  
57  
58  
59  
60  
61  
62  
63  
64  
65

According to the experimental protocol (

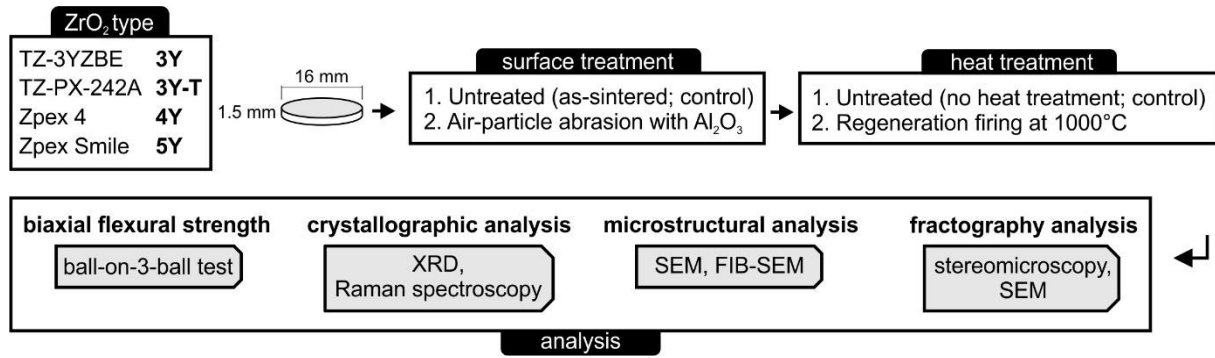
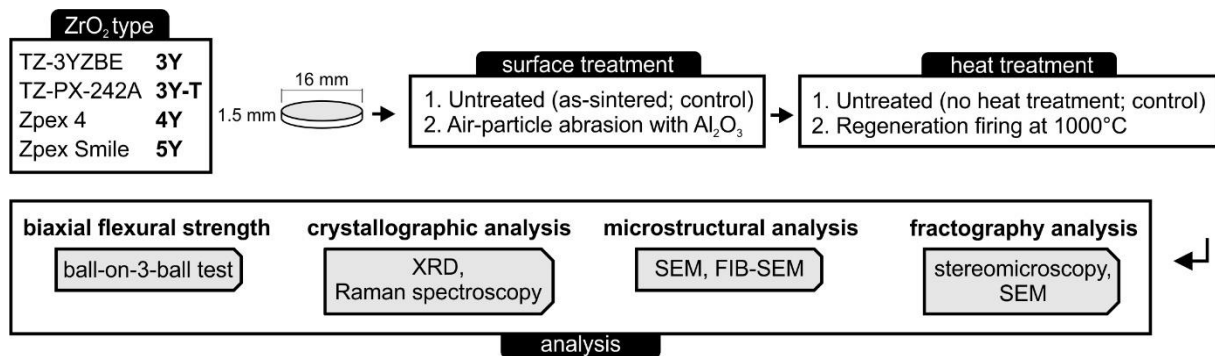


Figure 1), disc-shaped specimens were subjected to the following treatments:



**Figure 1.** Study design.

Half of the disc-shaped specimens of each zirconia group (3Y, 3Y-T, 4Y, 5Y) were airborne-particle abraded (APA) using 50  $\mu\text{m}$  Al<sub>2</sub>O<sub>3</sub> particles under controlled conditions and parameters at a pressure of 0.2 MPa for 10 s by using a custom-made APA device. The discs were mounted at a distance of 10 mm from the tip of the air-abrasion unit, equipped with a nozzle of 0.8 mm in diameter. A custom-made APA device was digitally designed and 3D printed with digital light processing technology (DLP) from acrylic polymer to precisely control the abrading distance and the vertical angulation of the handpiece during the procedure (**Error! Reference source not found.**, Supplementary Material). All the samples were ultrasonically cleaned in acetone, ethanol, and deionized water for 2 min in each solvent. Half of the samples were left in the as-sintered (AS) condition to serve as a control.

Half of the specimens from the AS and APA groups underwent subsequent heat treatment at 1000°C with a dwell time of 15 min and a heating rate of 100 °C/min (Programat X1, Ivoclar

Vivadent, Schaan, Lichenstein), also known as regeneration firing and designated as RF throughout the text.

## 2.2 Testing methods

### 2.2.1 Biaxial flexural strength

The biaxial flexural strength was measured in a universal material-testing machine (Quasar 2.5, Galdabini, Cardano al Campo, Italy) using the ball on three balls method (B3B) at ambient conditions (Fig. S2, Supplementary Material) [19]. The crosshead speed was 1 mm/min. The airborne particle abraded specimens were loaded with the treated side under tension. The failure stress of each tested specimen ( $\sigma_{max}$  in MPa) was calculated according to the following equation (1) [19]:

$$\sigma_{max} = f \frac{F}{t^2} \quad (1)$$

where  $F$  is the recorded load at fracture (in N),  $t$  is the thickness of the specimen (in mm), and  $f$  is a dimensionless factor that depends on the geometry of the sample, the Poisson's ratio  $\nu$  of the tested material, and the radius of the supporting ball.

### 2.2.2 Phase characterization

#### 2.2.2.1 X-ray diffractometry (XRD)

To determine the content of polymorphic zirconia crystalline phases, three randomly selected specimens from each group were submitted to crystallographic phase analysis by X-ray diffraction (XRD) using Cu-K $\alpha$  radiation over the range 25–40° (2 $\Theta$ ) at ambient temperature by automatic diffractometer (X'Pert PRO X-ray diffractometer, PANalytical, Almelo, Netherlands). A scanning step of 0.02° (2 $\Theta$ ) was adopted using step scanning mode. The amount of transformed monoclinic zirconia ( $X_m$ ) in APA specimens was estimated from the diffractograms using the Garvie and Nicholson equation [20].

#### 2.2.2.2 Raman spectroscopy

1 A WiTec Alpha 300 RA Raman Microscope (WITec GmbH, Ulm, Germany) with 532 nm  
2 excitation laser was used to analyze monoclinic, tetragonal, and cubic ZrO<sub>2</sub> of one out of 3Y-  
3 AS, 3Y-APA, 3Y-APA-RF, 3Y-T-APA, 4Y-APA, 5Y-AS and 5Y-APA specimens respectively.  
4 Laser intensity was set at 1.2 mW, resulting in optimal S-N ratio, while ensuring no local phase  
5 changes on the sites of measurement. A 100x (0.9 NA) objective was used to perform the  
6 measurements in a confocal setup, while the acquisition time was 20 s.  
7  
8  
9

### 10 11 *2.2.3 Microstructure analysis*

12 The examination of the specimen microstructure was performed using scanning electron  
13 microscopy (SEM) on the disc's surface after polishing and thermal etching (SEM; Carl Zeiss  
14 AG, Oberkochen, Germany). The grain size distributions were obtained from planimetric  
15 analyses of SEM micrographs (taking into account ~500 grains per sample) using ImageJ  
16 image-analysis software (Version 1.50b, 2015, Wayne Rasband, National Institutes of Health,  
17 Bethesda, MD, USA). Focused Ion Beam Microscopy (FIB, Carl Zeiss AG, Oberkochen,  
18 Germany) was employed to cut and polish a trench on the surface of APA specimens after  
19 depositing a 0.5 μm layer of protective platinum film, using ion beam machining at 30 kV and  
20 65 nA and finalized by ion polishing at 30 kV and 21 nA. The sub-surface cross-sections  
21 microstructure was then observed in situ, at an angle of 52° using the electron probe at 2 kV  
22 and 100 pA, by secondary electron (SE), in order to reveal the presence of phase  
23 transformation.  
24  
25  
26  
27  
28  
29  
30  
31  
32  
33  
34  
35  
36  
37  
38  
39  
40

### 41 *2.2.4 Fractography*

42 Fractographic analyses were performed to identify the location and size of the critical defects  
43 causing failure in the biaxial bending tested specimens [21]. Selected fracture surfaces of the  
44 broken disc specimens were sputtered with gold using an Agrar Sputter Coater and  
45 investigated using a SEM (JEOL JCM-6000Plus, Neoscope<sup>TM</sup>, JEOL Ltd., Tokyo, Japan).  
46  
47  
48  
49  
50

### 51 *2.3 Statistical analysis*

52 Statistical analysis was performed using statistical software (IBM SPSS Statistics, v27.0, IBM  
53 Corp, New York, USA). Levene's test of homogeneity was employed to determine the equality  
54 of variances. The biaxial flexural strength differences between treatment and types of zirconia  
55  
56  
57  
58  
59  
60  
61  
62  
63  
64  
65

1 groups were determined using one-way ANOVA followed with Tukey HSD *post hoc* test for  
2 pairwise comparison. The level of statistical significance was set at  $P < 0.05$ . Failure stress data  
3 from the B3B biaxial flexural test were analyzed in the framework of Weibull statistics [22]. The  
4 characteristic strength ( $\sigma_0$ ) and the Weibull modulus ( $m$ ) along with the corresponding 90%  
5 confidence intervals were obtained following the standards EN 843-5 [23]. The characteristic  
6 strength is the stress corresponding to a failure probability of ~63%, and the Weibull modulus  
7 is a measure of the underlying distribution of critical defects at the surface or in the volume of  
8 the material, and can be associated with the material's reliability.  
9  
10  
11  
12  
13  
14  
15

### 16 **3. Results**

#### 17 **3.1 Phase characterization**

##### 18 **3.1.1 XRD**

19 Representative XRD patterns of the AS and the APA groups are shown in Figure 2. All  
20 characteristic XRD peaks representing  $t$ -ZrO<sub>2</sub> are present in 3Y and 3Y-T specimens, whereas  
21 4Y and 5Y zirconia specimens were composed of mixed tetragonal ( $t$ -ZrO<sub>2</sub>) and  $t$ -prime ( $t'$ -  
22 ZrO<sub>2</sub>) phases, where the latter is tetragonal with a lower degree of tetragonality [24,25]. The  
23 XRD peaks corresponding to  $t$ -prime phases in 4Y and 5Y, (004)<sub>t'</sub> and (220)<sub>t'</sub>, can be observed  
24 in between the so-called  $t$ -ZrO<sub>2</sub> doublet peaks of the same crystal planes positioned around  
25 ~35° 2 $\Theta$  (Fig. 2a). This phenomenon is more distinctly observed in 5Y. In addition, slight  
26 shifting of (101)<sub>t/t'</sub> main peak at 30° 2 $\Theta$  can be observed for 5Y, since the (101) diffraction peak  
27 of  $t$ -prime,  $t$ -double-prime, and (111)<sub>c</sub> (pure cubic phase) are positioned at slightly lower 2 $\Theta$   
28 values (Fig. 2a and b). It is striking to observe the disappearance/annihilation of the  $t$ -prime  
29 doublet peaks for the 4Y specimen and increase of the intensity of (220)<sub>t</sub> peak after  
30 regeneration firing (Fig. 6b). APA influenced the XRD patterns of all zirconia ceramics by  
31 pronounced asymmetric low-2-theta broadening of the main (101)<sub>t/t'</sub> peak. The higher the  
32 yttrium concentration, the bigger the low-2-theta "hump" [26]. APA also significantly broadened  
33 the  $t$ -ZrO<sub>2</sub> (004) peaks, but not the (220)<sub>t</sub>. However, the reversed intensities of the (004)<sub>t/t'</sub> and  
34 (220)<sub>t/t'</sub> peaks are clearly evident. The lower the asymmetry of the crystal phase, the more  
35 pronounced the reversal of intensities occurred ( $t \rightarrow t'$ -prime  $\rightarrow t$ -double-prime-ZrO<sub>2</sub>) (Fig. 2c).  
36  
37  
38  
39  
40  
41  
42  
43  
44  
45  
46  
47  
48  
49  
50  
51  
52  
53  
54  
55  
56  
57  
58  
59  
60  
61  
62  
63  
64  
65

Only in the case of APA,  $m\text{-ZrO}_2$ ,  $(111)_m$  was detected in all the specimens, but at the absence of  $(002)_m$  peaks (Fig. 2c). The calculated XRD monoclinic fraction corresponded to  $X_m$  values of 4.7, 4.0, 1.8, and 0.5 % for the 3Y-APA, 3Y-T-APA, 4Y-APA, and 5Y-APA, respectively. Although the detection and calculation for the 5Y were obscure.

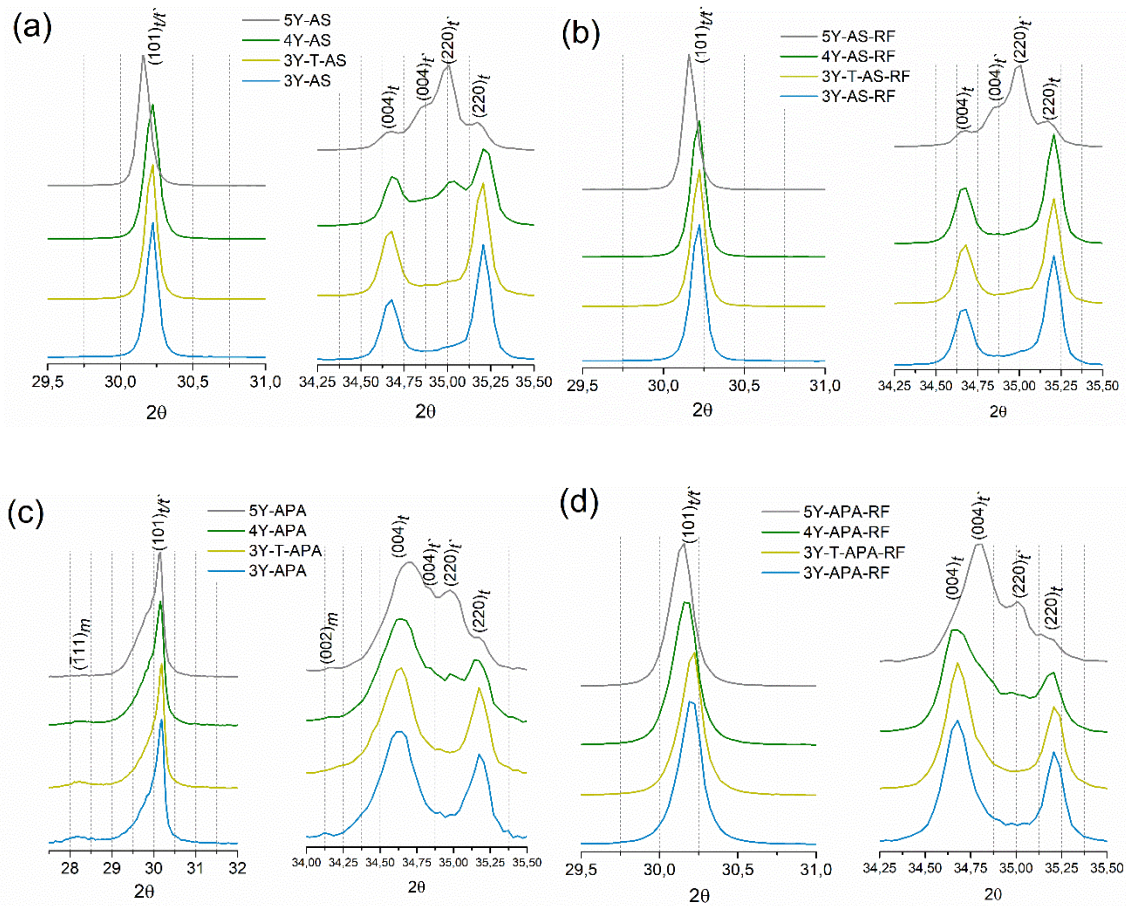


**Figure 2.** Representative XRD patterns of the zirconia specimens for as-sintered groups before (a) and after (b) regeneration firing and for APA groups before (c) and after (d) regeneration firing.

After submitting the APA zirconias to regeneration firing, the  $m\text{-ZrO}_2$  was reversed back to  $t\text{-ZrO}_2$ , whereas the reverse intensities of the  $(004)/(220)_{t/t}$  remained unchanged. The broadening of the  $(101)_{t/t}$  and  $(004)_{t/t}$  peaks was still evident but less pronounced. In addition, the reversed intensities of the  $(004)_{t/t}$  to  $(220)_{t/t}$  peaks remained unchanged (Fig. 2d).

### 3.1.2 Raman spectroscopy

Raman spectroscopy showed the presence of only tetragonal and cubic phases in as-sintered specimens (Fig. 3a). However, specimen 5Y-AS presented the highest peak shift in the 610-

640  $\text{cm}^{-1}$  to lower wavenumbers and an overall increase in signal intensity, indicating a higher fraction of cubic (or *t*-prime) phases. The depth profiles were analysed for determining the presence of the monoclinic phase. By comparing the characteristic peaks for tetragonal and monoclinic phases and their peak ratio, an evaluation of the amount and depth distribution of the latter was made. 3Y-APA, 3Y-T-APA, and 4Y-APA specimens revealed the presence of the monoclinic phase in the top surface layer, which gradually decreased from surface to  $\sim 2$   $\mu\text{m}$  below the sample's surface, indicating that the surface tetragonal phase transformed into a monoclinic phase with APA (Fig. 3c). In 5Y-APA no clear detection of the monoclinic peaks was observed. However, after regeneration firing the monoclinic phase in APA specimens was completely reverted back to tetragonal phase (Fig. 3b), corroborating with the XRD results (Fig. 2).

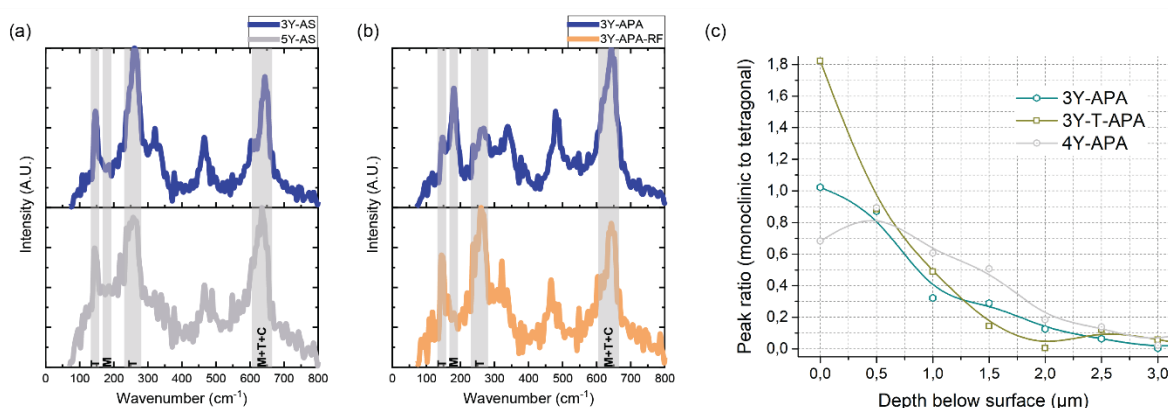


**Figure 3.** Raman spectra for (a) as-sintered 3Y and 5Y and (b) 3Y-APA and 3Y-APA-RF specimens showing characteristic peaks of tetragonal, monoclinic and cubic (*t*-prime) zirconia phases. (c) The depth profile ratio between the monoclinic and tetragonal phases based on the peaks at 180 and 265  $\text{cm}^{-1}$  for the 3Y-APA, 3Y-T-APA, and 4Y-APA zirconia ceramic.

### 3.2 Microstructure SEM analysis

The microstructure of the zirconia ceramics revealed polycrystalline and dense structures with the presence of only few pores. The four zirconia ceramics differed in microstructure with respect to the grain size (Fig. 4). The size of the zirconia grains increased with the amount of yttria; the largest grains were observed in the 5Y group. Grain size distributions (GSDs) were determined, and the results are presented in Figure S3 and Table S2 (Supplementary

Material). 3Y has a typical GSD encountered in 3Y-TZP materials with a  $d_{50}$  value of 0.31  $\mu\text{m}$ . 3Y-T possessed an even narrower GSD and smaller  $d_{50}$  value of 0.28  $\mu\text{m}$ , where 90 % of grains ( $d_{90}$ ) were even smaller than 0.5  $\mu\text{m}$ . 4Y had a similar microstructure to 3Y materials and comparable grain sizes (Table S2), but as seen in GSD (Fig. S3), a small fraction of larger grains ( $>1 \mu\text{m}$ ) could already be detected. As expected, 5Y showed much broader GSD with a long tail of small fractions of bigger grains having a  $d_{50}$  value of 0.53  $\mu\text{m}$ .

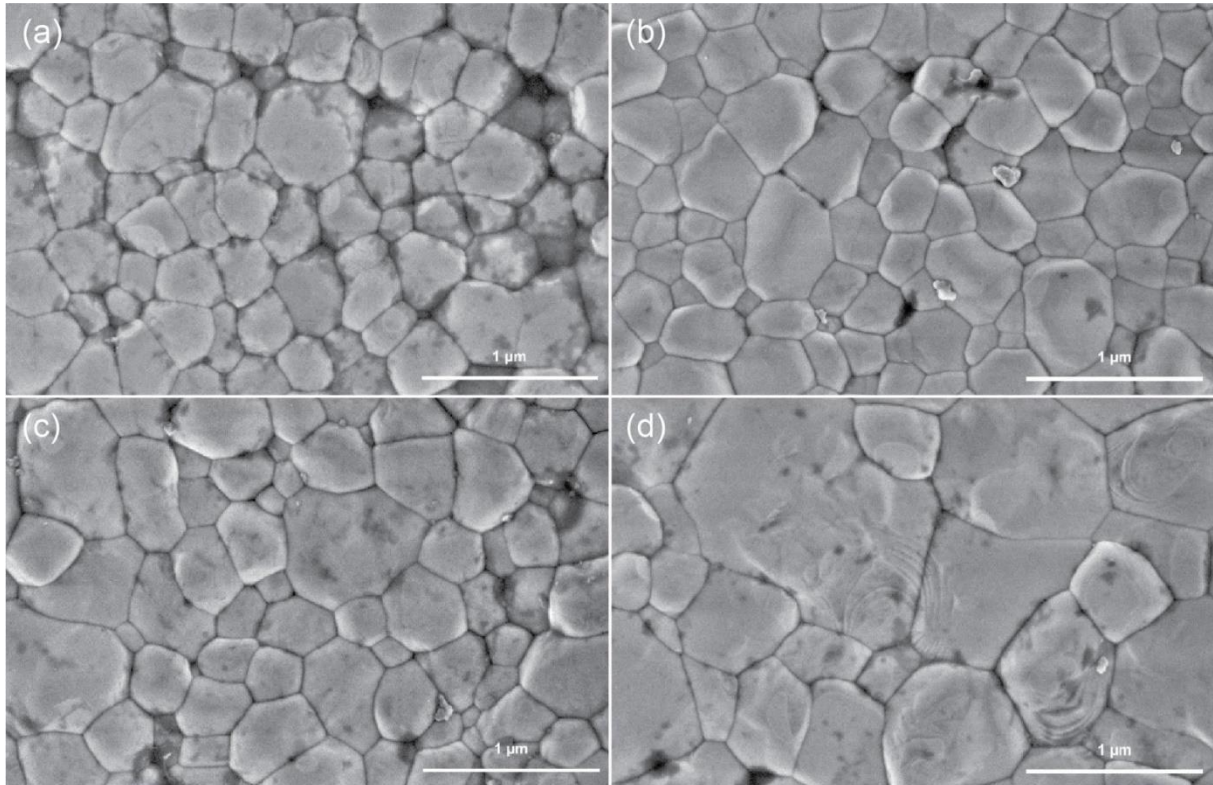
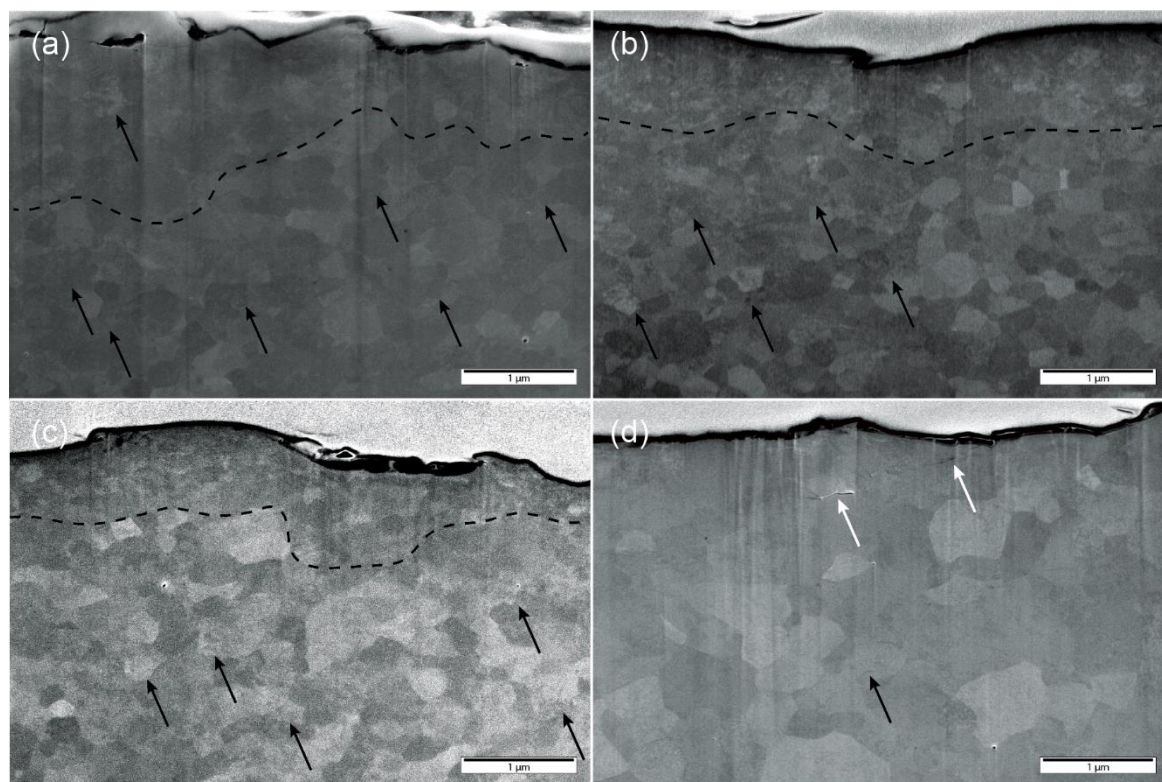


**Figure 4.** SEM micrographs of AS zirconias surfaces showing microstructures of (a) 3Y, (b), 3Y-T, (c) 4Y and (d) 5Y specimen.

### 3.3 FIB-SEM analysis

The extent of subsurface damage after APA was evaluated by FIB-SEM (Fig. 5). It revealed the in-depth fine-grain microstructure of zirconia materials. In the topmost 1  $\mu\text{m}$ , severe plastic-like deformation of 3Y-APA, 3Y-T-APA, and 4Y-APA material is evident, and the grains are refined, with no discernible boundaries between them. At depths between 1  $\mu\text{m}$  and 6  $\mu\text{m}$ , individual grains can be discriminated and appear to be deformed and cleaved apart. Distinct intra-granular boundaries and contrast heterogeneities resemble multiple newly-formed

1 domains, that according to Raman spectra cannot be ascribed to the monoclinic phase (Figs.  
2 3b-c). The depth below 6  $\mu\text{m}$  also shows shadows and cleavages in individual grains, albeit  
3 less prominently and with no clear transition boundary. The transformation zone depth in 5Y  
4 material could not be observed (Fig. 5), which agrees with the XRD results (Fig. 2). The FIB-  
5 SEM subsurface analysis of the 5Y-APA material showed multiple few lateral microcracks  
6 several micrometers long (Fig. 5).  
7  
8  
9  
10



39 **Figure 5.** FIB-SEM micrographs presenting APA zirconia specimens, i.e., (a) 3Y, (b), 3Y-T, (c)  
40 4Y and (d) 5Y specimen. Black dashed lines on images 3Y, 3Y-T, and 4Y indicate the severe  
41 plastically deformed topmost layer and transitions into a layer of altered grains. The white  
42 arrows indicate microcracks, while the black arrows indicate distinct shadows and the cleaved-  
43 like appearance of the grains. With depth, these changes gradually become less pronounced.  
44  
45  
46  
47  
48  
49  
50  
51 No plastic deformation of the topmost layer is observed in 5Y material.  
52

### 53 3.4 Biaxial flexural strength distributions

54  
55 Figures 6a and 6b show the probability of failure versus failure stress of the different samples  
56 in a Weibull diagram, without or with regeneration firing, respectively. Mean flexural strength  
57 values of the 3Y, 3Y-T, 4Y, and 5Y zirconia ceramic specimens and Weibull parameters are  
58  
59  
60  
61  
62  
63  
64  
65

presented in Table 1. Compared to group 3Y, the strength of groups 3Y-T, 4Y, and 5Y decreased by ~10%, ~20%, and ~40%, respectively. After the APA, mean flexural strengths of 3Y, 3Y-T, and 4Y groups increased to 1477 MPa (~25%), 1518 MPa (~40%), and 1131 MPa (~20%), respectively. On the other hand, the strength decreased for the 5Y group to 426 MPa (~40%) (Table 1). The differences between the AS and APA group were statistically significant for all zirconia specimens ( $P < 0.05$ ).

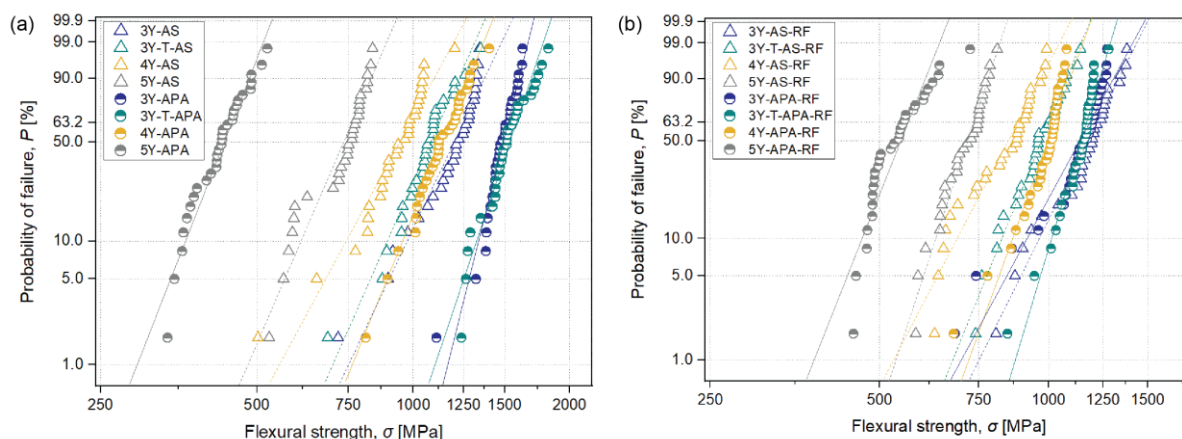


**Figure 6.** Probability of failure ( $P$ ) versus failure stress ( $\sigma$ ) for AS and APA groups of zirconia ceramics (a) without and (b) with regeneration firing.

After subjecting the AS and APA specimens to regeneration firing, the mean flexural strength significantly decreased for all specimen groups, except for the 5Y APA group, where the strength increased (Table 1). The most significant decreases were observed in APA groups, the highest in 3Y APA and 3Y-T APA specimens ( $P < 0.05$ , Table 1). In contrast, the differences in flexural strength between the AS groups were minimal and statistically insignificant, nearly maintaining values obtained before heat treatment.

**Table 1.** Biaxial flexural strength and Weibull parameters.

Treatment	Flexural strength ( $\sigma$ ) [MPa] <sup>A</sup>	Characteristic strength ( $\sigma_e$ ) [MPa] <sup>B</sup>	Weibull modulus ( $m$ ) <sup>B</sup>
AS	1184 (152) <sup>a</sup>	1241 [1206-1278]	12 [9-14]
3Y	AS+RF	1164 (146) <sup>ac</sup>	1223 [1185-1263]
	APA	1477 (104) <sup>b</sup>	1520 [1493-1547]

	APA+RF	1120 (146) <sup>ad</sup>	1174 [1141-1208]	12 [9-15]
	AS	1069 (133) <sup>cd</sup>	1125 [1084-1167]	9 [7-11]
3Y-T	AS+RF	959 (101) <sup>e</sup>	1003 [974-1033]	11 [8-14]
	APA	1518 (151) <sup>b</sup>	1586 [1539-1635]	11 [8-13]
	APA+RF	1127 (87) <sup>ac</sup>	1162 [1141-1185]	18 [13-22]
	AS	928 (133) <sup>ef</sup>	980 [943-1018]	9 [7-11]
4Y	AS+RF	835 (113) <sup>f</sup>	882 [851-913]	9 [7-12]
	APA	1130 (130) <sup>ac</sup>	1186 [1147-1227]	10 [8-12]
	APA+RF	979 (89) <sup>de</sup>	1012 [993-1032]	18 [13-22]
	AS	726 (89) <sup>h</sup>	763 [741-785]	12 [9-14]
5Y	AS+RF	709 (62) <sup>h</sup>	736 [719-753]	14 [11-18]
	APA	426 (49) <sup>g</sup>	447 [432-463]	10 [7-12]
	APA+RF	540 (65) <sup>i</sup>	570 [546-594]	8 [6-10]

n = 30 for each group

<sup>A</sup> Mean value of biaxial flexural strength with standard deviation.

<sup>B</sup> The characteristic strength and the Weibull modulus with the corresponding 90%-confidence intervals of the different specimen groups.

The same lower case letters written as superscripts of mean flexural strength values designate no statistical significance ( $P > 0.05$ ).

The Weibull analysis revealed higher characteristic strength of the APA groups than of the AS groups, except for the group 5Y, where the trend was opposite (Table 1). The lowest Weibull modulus was obtained for the 5Y APA-RF zirconia ceramics, whereas the highest was found in the 3Y-APA zirconia ceramics.

Treatment with APA significantly increased the Weibull moduli of 3Y, 3Y-T, and 4Y zirconia ceramics; the highest increase was observed in the group 3Y (from  $m=12$  to  $m=19$ ) and the

1 lowest in the group 4Y (from  $m=9$  to  $m=10$ ) (Table 1). After APA, the Weibull modulus of 5Y  
2 zirconia decreased (from  $m=12$  to  $m=10$ ).

3 Following the regeneration firing of zirconia specimens, no significant alterations of Weibull  
4 moduli were observed. The regeneration firing of AS groups 3Y-T, 4Y, and 5Y slightly  
5 increased Weibull moduli; the highest increase was obtained for the group 5Y (from  $m=12$  to  
6  $m=14$ ), whereas for the 3Y AS group, the Weibull modulus decreased (from  $m=12$  to  $m=11$ ).  
7 For the 3Y-T and 4Y APA groups, the Weibull moduli moderately increased, while for the 3Y  
8 and 5Y APA groups, the Weibull moduli decreased ( $m=19$  to  $m=12$  and  $m=10$  to  $m=8$ ,  
9 respectively) (Table 1, Fig. 2 and 3).  
10  
11  
12  
13  
14  
15  
16  
17  
18  
19

### 20 3.5 Fractographic analysis

21 Fractographic analysis on selected specimens was performed to study the typical flaws and/or  
22 defect origins that caused failure under monotonic loading with the B3B test. The most  
23 common flaw observed was in the form of a pre-notch-like intragranular pore or crack  
24 positioned normal to the specimen surface with the typical size of 10–20  $\mu\text{m}$  in size, likely  
25 originating from the incompletely deformed granules during dry pressing (Fig. 7). These types  
26 of flaws were detected in all zirconia types and specimen treatments. Several of the specimens  
27 from the APA groups fractured from larger flaws, 20–30  $\mu\text{m}$  in size, such as lateral cracks,  
28 alumina debris inclusion and/or imprints (or surface chip-outs), possibly as a result of the air-  
29 particle abrasion process (Fig. 8).  
30  
31  
32  
33  
34  
35  
36  
37  
38  
39  
40  
41  
42  
43  
44  
45  
46  
47  
48  
49  
50  
51  
52  
53  
54  
55  
56  
57  
58  
59  
60  
61  
62  
63  
64  
65

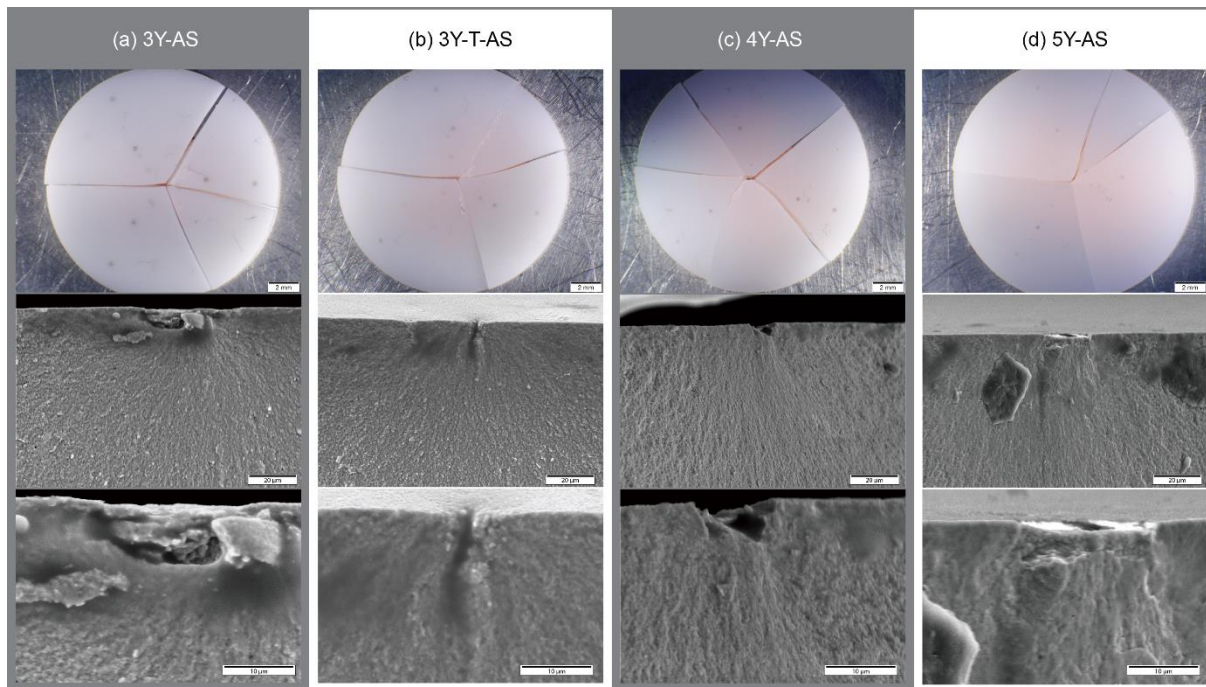


**Figure 7.** SEM fractographic analysis of the as-sintered (AS) zirconia specimens exhibiting critical flaws of similar size in the likes of cracks or pre-notches likely originating from incomplete pressing/demoulding: a) 3Y-AS ( $\sigma_{\max}$ =894 MPa), b) 3Y-T-AS ( $\sigma_{\max}$ =889 MPa) c) 4Y-AS ( $\sigma_{\max}$ = 822 MPa) and d) 5Y-AS ( $\sigma_{\max}$ =528 MPa).

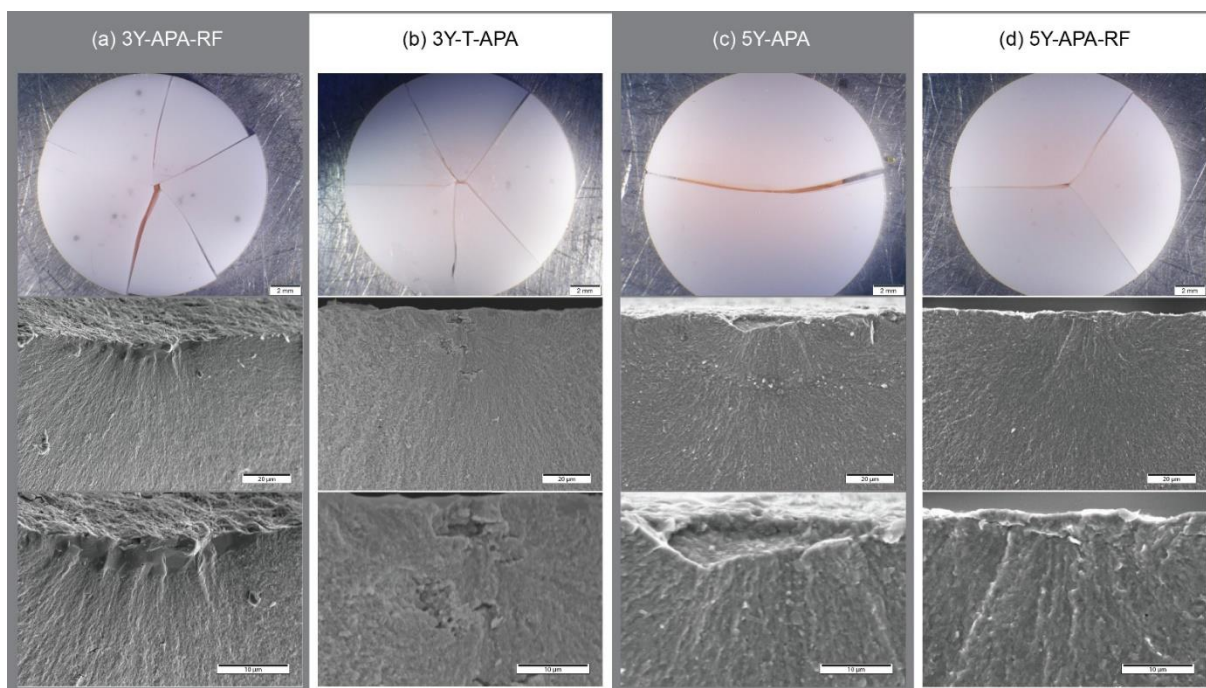


**Figure 8.** SEM fractographic analyses of the air-particle abraded (APA) zirconia specimens exhibiting critical flaws such as alumina particulate inclusions, imprints or subsurface lateral

cracks, as a result of the APA process: a) 3Y-T-APA ( $\sigma_{\max}=1263$  MPa), b) 3Y-APA-RF ( $\sigma_{\max}=742$  MPa) c) 5Y-APA ( $\sigma_{\max}=359$  MPa) and d) 5Y-APA-RF ( $\sigma_{\max}=486$  MPa).

#### 4. Discussion

Air-particle abrasion (APA) is a universally accepted dental laboratory surface treatment in prosthetic dentistry to clean and promote surface bonding of zirconia dental restorations. However, APA introduces surface irregularities, which may increase the probability of crack initiation in the ceramic part. The present study investigated the effects of APA-surface-roughening of yttria-containing zirconia on its mechanical integrity and the effects of additional regeneration firing (RF) after APA to reverse the  $m \rightarrow t$  phase transformation process. Our findings showed that the effect of APA on different generations of dental zirconia ceramics was ambivalent. APA significantly increased the flexural strength of traditional 3Y ceramics as well as of a more translucent variant, i.e. 3Y-T. However, the flexural strength of ultra-translucent (5Y) zirconia ceramics significantly decreased after APA. Likewise, the effects of RF on the structural and crystallographic stability of novel translucent zirconia ceramics were comprehensively considered. The RF reversed the effect of APA, hence lowering the flexural strength of 3Y, 3Y-T, and 4Y ceramics and enhancing the strength of 5Y ceramics. To the authors' knowledge, the present study declares the first comparison of the effects of APA before and after RF for every generation of zirconia dental ceramic available at present.

The  $t \rightarrow m$  transformation toughening in zirconia is bounded to the amount of tetragonal phase and also to the crystal tetragonality of the phases. In the present study, it has been shown that the ZrO<sub>2</sub> with a higher amount of yttria presented inferior mechanical integrity. Thus, 4Y had a less toughening effect than 3Y and 3Y-T, whereas, for 5Y, the  $t \rightarrow m$  transformation was almost completely lost. At the same time, the lower crack growth resistance of translucent zirconia raises another concern in terms of surface treatments such as APA. For example, APA is able to enhance the strength of 3Y-TZP apparently due to the generation of micro-residual compressive stresses generated by ~5 vol.% increase that accompanies martensitic  $t \rightarrow m$  phase transformation [13,27,28]. However, this effect might be compromised in partially stabilized cubic zirconias (4Y-PSZ and 5Y-PSZ) [29]. The APA surface pre-treatment at a

1 milder pressure of 0.2 MPa was employed here since it was previously shown to provide a  
2 reliable and durable bonding of zirconia to resin cement [30–32].

3 The improvement of the flexural strength of 3Y, 3Y-T, and 4Y zirconia after APA has been  
4 related to the microstructural and crystallographic changes observed with FIB-SEM, XRD and  
5 Raman analysis (Figs. 2, 3 and 5). 3Y, 3Y-T, and 4Y APA abraded specimens showed  
6 distinctly altered microstructure, reaching the transformation zone depth (TZD) about 10  $\mu\text{m}$   
7 below the surface with evident severe plastic deformation of the topmost  $\sim 1 \mu\text{m}$  layer and grain  
8 reorientation (Fig. 5). The APA induced the  $t \rightarrow m$  transformation of the zirconia grains in 3Y,  
9 3Y-T, and 4Y material  $\sim 2 \mu\text{m}$  below the surface, which was confirmed with Raman  
10 spectroscopy analysis (Fig. 3). Likewise, a high distortion of the XRD peaks and reversal of  
11 intensities were observed and accompanied by the emergence of a small amount of monoclinic  
12 phase detected after APA. Furthermore, the flexural strength of 4Y material slightly increased  
13 after APA but significantly decreased in 5Y material (Table 1), supporting the observation that  
14 some  $t \rightarrow m$  toughening effect is still present in 4Y zirconia and presumably lost in 5Y zirconia  
15 [7]. Nevertheless, observing the presence of the monoclinic phase residues in the XRD pattern  
16 (Fig. 2b) in 5Y after APA is not in line with some previous studies [9]. However, it should be  
17 emphasized that the possible  $t \rightarrow m$  transition process in the 5Y material appears to be  
18 insufficient to compress the APA introduced subsurface microcracks (Fig. 5), leading to  
19 reduced strength of the material. Fractographic analysis showed bigger flaws (chip-outs and  
20 lateral crackings) in 5Y, obviously resulting in more brittle specimens (Figs. 9c-d). The  
21 damaging effect of APA in the 5Y material was also observed in some previous studies [10,15],  
22 showing that even low-pressure abrasion (0.1 MPa) leads to strength degradation.

23 The conditions of RF used in the present study are recommended by the manufacturer for 3Y-  
24 TZP, when the laboratory adjustment and grinding of zirconia material are performed, where  
25 the material is submitted to 1000°C for 15 minutes. Regardless of the holding time, heat  
26 initiates the reverse ( $m \rightarrow t$ ) transformation, eliminates the monoclinic phase from the material  
27 surface, relieves the created compressive stresses, and reduces the strength of the material.  
28 RF of APA specimens completely reversed phases ( $m \rightarrow t$ ) (Fig. 2). Realizing that compressive  
29 residual stresses are relaxed with  $m \rightarrow t$  transition [33], the mechanical strength is hence merely  
30  
31  
32  
33  
34  
35  
36  
37  
38  
39  
40  
41  
42  
43  
44  
45  
46  
47  
48  
49  
50  
51  
52  
53  
54  
55  
56  
57  
58  
59  
60  
61  
62  
63  
64  
65

1 related to the APA-introduced flaws or defects [13]. The flexural strengths of the 3Y-APA, 3Y-  
2 T-APA, and 4Y-APA specimens dropped significantly after RF (Table 1), but were not lower  
3 than that of as-sintered specimens. One would expect that flaws induced by APA, such as  
4 lateral subsurface cracks and alumina particle inclusions (Figs. 9a-b) would be responsible for  
5 a more significant strength degradation if not counteracted by the persistent surface layer of  
6 micro residual compressive stresses. When the as-sintered (AS) specimens sustained the RF,  
7 the flexural strength was nearly retained, and the intensities of crystal phases were unchanged,  
8 showing no preceding residual stresses present in the control material. However, when  
9 comparing the APA abraded 3Y, 3Y-T, and 4Y zirconia ceramics treated with RF to AS  
10 counterparts, the flexural strength of APA specimens even slightly exceeded the values of the  
11 AS samples (Table 1).  
12  
13  
14  
15  
16  
17  
18  
19  
20  
21  
22

23 After RF of all the APA specimens, the intensities of  $I_t(002)/I_t(110)$  remained reversed (Fig. 2),  
24 which indicates on the possibility that some micro-residual compressive stresses were not  
25 relaxed [34]. This could well corroborate with distinct intra-granular boundaries and contrast  
26 heterogeneities observed with FIB-SEM in depth between 1  $\mu\text{m}$  and 6  $\mu\text{m}$  (Fig. 5). The  
27 reversed intensities of  $I_t(002)/I_t(110)$  were assigned to the formation of coercive stresses from  
28 ferroelastic domain (FE) switching in tetragonal prime ( $t'$ ) zirconia, which is known to occur as  
29 a result of externally applied mechanical stresses (APA) and shows only weak temperature  
30 and strain-rate dependence [35,36]. It could explain the remarkably high flexural strengths of  
31 regeneration-fired APA specimens with a high degree of surface damage (Figs. 9a-b) but still  
32 equalling (or even surpassing) the strengths of AS specimens with similar or smaller critical  
33 flaws responsible for fracture (Figs. 8a-b).  
34  
35  
36  
37  
38  
39  
40  
41  
42  
43  
44  
45  
46  
47  
48

49 In the 5Y-APA material, where minimal compressive stresses were generated at the surface  
50 layers owing to the  $t \rightarrow m$  transformation, the flexural strength significantly increased after RF  
51 although not reaching the AS values, which is in line with some previous studies [15]. Ho and  
52 co-workers found that regeneration firing of 3Y-TZP can decrease the extension of the cracks,  
53 which was also suggested in the study of Hatanaka et al., where the maintenance of the  
54  
55  
56  
57  
58  
59  
60  
61  
62  
63  
64  
65

flexural strength of the zirconia after regeneration firing was explained by the interaction of reverse  $m \rightarrow t$  phase transformation and crack healing [17].

The reliability of the material has been discussed in terms of the Weibull modulus. The increasing yttria content did not affect the mechanical reliability, as opposed to the findings of the study of Zhang *et al.*, where the decreased reliability was attributed to the reduced crack-growth resistance and thus higher sensitivity to cracks/defects [7]. APA, along with increasing characteristic strength, slightly increased the reliability of the 3Y, 3Y-T, and 4Y zirconia materials. The same was not observed for the 5Y material ( $m=10$ ), where the characteristic strength was considerably deprived after APA (762 MPa to 447 MPa). However, the mean strength of 5Y-APA (425 MPa) still reached the values of other non-oxide translucent ceramics such as lithium disilicate (428 MPa) [37]. It is worth highlighting the increase in Weibull moduli after RF in all zirconia groups, except for the 3Y and air-abraded 5Y material. The enhanced reliability of 3Y-TZP after RF was also shown in a previous study [17].

In summary, the Weibull moduli determined in this study ranged between  $m=10$  and  $m=19$  (Table 1). In general,  $m$  for all the groups was around 10, with the exception of specimens groups 3Y-APA, 3Y-T-APA-RF, 4Y-APA-RF, and 5Y-AS-RF, which had exceptionally higher  $m$  of 19, 18, 18, and 14, respectively. In the case of 3Y zirconia, the APA increases  $m$  significantly. This may be associated with the effect of pressure on the surface, thus "eliminating" some relatively large defects. In the case of 3Y-T, 4Y, and 5Y, however, the increase in  $m$  is observed after the RF treatment. The fractographic analysis revealed that the presence of processing related defects in all specimens, such as pre-notch-like intragranular pore or cracks, uplifts and imprints as a result of incomplete pressing/demoulding likely originating from the incompletely deformed granules during dry pressing, was ultimate defining merit for the final Weibull modulus of the group. The characteristic strength in the AS specimens, however, was insensitive to these flaws, but was governed by the toughening ability of different zirconia generation. In the case of APA groups, flaw types of lateral microcracking or alumina grain inclusion (Figs 9-ab) could be assigned to the process of APA, but their occurrence was low, or the flaw-type could not outplay the benefit of compressive stresses introduced by the APA process. This finding advocates the employment of APA.

1  
2  
3  
4  
5  
6  
7  
8  
9  
10  
11  
12  
13  
14  
15  
16  
17  
18  
19  
20  
21  
22  
23  
24  
25  
26  
27  
28  
29  
30  
31  
32  
33  
34  
35  
36  
37  
38  
39  
40  
41  
42  
43  
44  
45  
46  
47  
48  
49  
50  
51  
52  
53  
54  
55  
56  
57  
58  
59  
60  
61  
62  
63  
64  
65

Caution should be taken when considering the 5Y dental zirconia. By the findings of this study, APA with or without further RF would significantly decrease the strength of the material and slightly decrease the Weibull modulus. More severe flaws after APA were found in 5Y specimens (Figs 9c-d) possibly associated with the brittleness of the 5Y. For conventional 3Y and highly translucent 4Y dental zirconia, even though the RF treatment unleashed the APA's  $t \rightarrow m$  strengthening effect, RF can still be considered to be a beneficial treatment as it again generates more reliable zirconia material. It can be summarised that the reliability of zirconia dental ceramics is governed by the type used (yttria content) and by the post-manufacturing steps employed, such as APA and RF. Reliability directly translates into employing clinical recommendations.

## Conclusions

The present study showed that the APA toughening of tetragonal rich zirconia, 3Y-TZP and 4Y-PSZ, is related to  $t \rightarrow m$  transformation strengthening and ferroelastic (FE) domain switching phenomenon. After regeneration firing, the latter is presumably the persisting mechanism to withstand the propagation of APA-induced cracks, reinforcing the 3Y-TZP and 4Y-PSZ zirconia ceramic. It should be emphasized that the damaging effects of APA might be critically more important when dental restorations are produced entirely from full-contour monolithic zirconia stabilized with 5 mol.% of yttria. Therefore, the clinical recommendation to avoid post-sintering adjustments of 5Y-PSZ ceramics, including APA surface roughening, can be proposed. Alternative non-invasive surface pre-treatments to enhance the adhesion of 5Y-PSZ should be employed instead. Furthermore, if surface adjustments of 5Y-PSZ are needed, the concurrent use of heat treatment in terms of regeneration firing can be endorsed.

## Acknowledgments

This work was supported by the Slovenian Research Agency funding through research projects Towards reliable implementation of monolithic zirconia dental restorations (J2-9222) and Preclinical and clinical investigations of zirconia dental ceramics fabricated by additive manufacturing technologies (J3-3064), and research programs Ceramics and complementary materials for advanced engineering and biomedical applications (P2-0087) and Advanced

materials for low-carbon and sustainable society (P2-0393). The authors would like to thank Irina Kraleva, from the Chair of Structural and Functional Ceramics, at the Montanuniversität Leoben, for the assistance with the fractographic analysis.

## Literature

- [1] R. Garvie, R. Hannink, R. Pascoe, Ceramic steel?, *Nature*. 258 (1975) 703–704. <http://www.nature.com/nature/journal/v258/n5537/abs/258703a0.html> (accessed November 12, 2013).
- [2] E. Camposilvan, R. Leone, L. Gremillard, R. Sorrentino, F. Zarone, M. Ferrari, J. Chevalier, Aging resistance, mechanical properties and translucency of different yttria-stabilized zirconia ceramics for monolithic dental crown applications, *Dent. Mater.* 34 (2018) 879–890. <https://doi.org/10.1016/j.dental.2018.03.006>.
- [3] A. Kocjan, J. Cotič, T. Kosmač, P. Jevnikar, In vivo aging of zirconia dental ceramics – Part I: Biomedical grade 3Y-TZP, *Dent. Mater.* 37 (2021) 443–453. <https://doi.org/10.1016/j.dental.2020.11.023>.
- [4] J. Cotič, A. Kocjan, S. Panchevska, T. Kosmač, P. Jevnikar, In vivo ageing of zirconia dental ceramics — Part II: Highly-translucent and rapid-sintered 3Y-TZP, *Dent. Mater.* 37 (2021) 454–463. <https://doi.org/10.1016/j.dental.2020.11.019>.
- [5] J.F. Güth, B. Stawarczyk, D. Edelhoff, A. Liebermann, Zirconia and its novel compositions: What do clinicians need to know?, *Quintessence Int.* 50 (2019) 512–520. <https://doi.org/10.3290/j.qi.a42653>.
- [6] A. Kocjan, T. Mirt, R.-J. Kohal, Z. Shen, P. Jevnikar, Zirconia Ceramics: Clinical and Biological Aspects in Dentistry, in: M. (ed) Pomeroy (Ed.), *Encycl. OfMaterials Tech. Ceram. Glas., Oxford: Elsevier, 2021: pp. 817–832*. <https://doi.org/10.1179/mst.1985.1.6.417>.
- [7] F. Zhang, H. Reveron, B.C. Spies, B. Van Meerbeek, J. Chevalier, Trade-off between fracture resistance and translucency of zirconia and lithium-disilicate glass ceramics for monolithic restorations, *Acta Biomater.* 91 (2019) 24–34.

<https://doi.org/10.1016/j.actbio.2019.04.043>.

- 1 [8] S.J. Kwon, N.C. Lawson, E.E. McLaren, A.H. Nejat, J.O. Burgess, Comparison of the  
2 mechanical properties of translucent zirconia and lithium disilicate, *J. Prosthet. Dent.*  
3 120 (2018) 132–137. <https://doi.org/10.1016/j.prosdent.2017.08.004>.  
4  
5  
6  
7  
8 [9] M. Inokoshi, H. Shimizu, K. Nozaki, T. Takagaki, K. Yoshihara, N. Nagaoka, F. Zhang,  
9 J. Vleugels, B. Van Meerbeek, S. Minakuchi, Crystallographic and morphological  
10 analysis of sandblasted highly translucent dental zirconia, *Dent. Mater.* 34 (2018) 508–  
11 518. <https://doi.org/10.1016/j.dental.2017.12.008>.  
12  
13  
14  
15  
16  
17 [10] E.A. McLaren, N. Lawson, J. Choi, J. Kang, C. Trujillo, New High-Translucent Cubic-  
18 Phase-Containing Zirconia: Clinical and Laboratory Considerations and the Effect of Air  
19 Abrasion on Strength., *Compend. Contin. Educ. Dent.* 38 (2017) e13–e16.  
20  
21  
22  
23  
24  
25 [11] T. Malgaj, A. Plut, A. Eberlinc, M. Drevenšek, P. Jevnikar, Anterior Esthetic  
26 Rehabilitation of an Alveolar Cleft Using Novel Minimally Invasive Prosthodontic  
27 Techniques: A Case Report, *Cleft Palate-Craniofacial J.* (2020) 1055665620964709.  
28 <https://doi.org/10.1177/1055665620964709>.  
29  
30  
31  
32  
33  
34  
35 [12] M. Kern, S.M. Wegner, Bonding to zirconia ceramic: Adhesion methods and their  
36 durability, *Dent. Mater.* 14 (1998) 64–71. [https://doi.org/10.1016/S0109-5641\(98\)00011-6](https://doi.org/10.1016/S0109-5641(98)00011-6).  
37  
38  
39  
40  
41  
42 [13] T. Kosmač, Č. Oblak, P. Jevnikar, N. Funduk, L. Marion, The effect of surface grinding  
43 and sandblasting on flexural strength and reliability of Y-TZP zirconia ceramic, *Dent.*  
44 *Mater.* 15 (1999) 426–433. [https://doi.org/10.1016/0038-1101\(68\)90151-2](https://doi.org/10.1016/0038-1101(68)90151-2).  
45  
46  
47  
48  
49 [14] J. Cotič, P. Jevnikar, A. Kocjan, Ageing kinetics and strength of airborne-particle  
50 abraded 3Y-TZP ceramics, *Dent. Mater.* 33 (2017) 847–856.  
51 <https://doi.org/10.1016/j.dental.2017.04.014>.  
52  
53  
54  
55  
56  
57 [15] K. Yoshida, Influence of alumina air-abrasion for highly translucent partially stabilized  
58 zirconia on flexural strength, surface properties, and bond strength of resin cement, *J.*  
59 *Appl. Oral Sci.* 28 (2020) 1–9. <https://doi.org/10.1590/1678-7757-2019-0371>.  
60  
61  
62  
63  
64  
65

- 1  
2  
3  
4  
5  
6  
7  
8  
9  
10  
11  
12  
13  
14  
15  
16  
17  
18  
19  
20  
21  
22  
23  
24  
25  
26  
27  
28  
29  
30  
31  
32  
33  
34  
35  
36  
37  
38  
39  
40  
41  
42  
43  
44  
45  
46  
47  
48  
49  
50  
51  
52  
53  
54  
55  
56  
57  
58  
59  
60  
61  
62  
63  
64  
65
- [16] D.P.O. Ryan, L.M.G. Fais, S.G. Antonio, G.R. Hatanaka, L.M. Candido, L.A.P. Pinelli, Y-TZP zirconia regeneration firing: Microstructural and crystallographic changes after grinding, *Dent. Mater. J.* 36 (2017) 447–453. <https://doi.org/10.4012/dmj.2016-124>.
- [17] G.R. Hatanaka, G.S. Polli, L.M.G. Fais, J.M. dos S.N. Reis, L.A.P. Pinelli, Zirconia changes after grinding and regeneration firing, *J. Prosthet. Dent.* 118 (2017) 61–68. <https://doi.org/10.1016/j.prosdent.2016.09.026>.
- [18] G.S. Polli, G.R. Hatanaka, F.D.O. Abi-rached, M. de S. Goez, J.M. dos S.N. Reis, Fatigue behavior and surface characterization of a Y-TZP after laboratory grinding and regeneration firing, *J. Mech. Behav. Biomed. Mater.* 88 (2018) 305–312. <https://doi.org/10.1016/j.jmbbm.2018.08.019>.
- [19] A. Börger, P. Supancic, R. Danzer, The ball on three balls test for strength testing of brittle discs: stress distribution in the disc, *J. Eur. Ceram. Soc.* 22 (2002) 1425–36. <https://doi.org/10.1016/j.jeurceramsoc.2003.10.035>.
- [20] R. Garvie, P. Nicholson, Structure and Thermomechanical Properties of Partially Stabilized Zirconia in the CaO-ZrO<sub>2</sub> System, *J. Am. Ceram. S.* 55 (1972) 152–157. <http://onlinelibrary.wiley.com/doi/10.1111/j.1151-2916.1972.tb11241.x/abstract> (accessed April 19, 2013).
- [21] G. Quinn, NIST Recommended Practice Guide: Fractography of Ceramics and Glasses, 2nd edition, (2016). <https://doi.org/https://doi.org/10.6028/NIST.SP.960-16e2>.
- [22] W. Weibull, A Statistical Distribution Function of Wide Applicability, *J. Appl. Mech.* Vol. 18 (1951) 293–297.
- [23] EN 843-5, Advanced technical ceramics - Mechanical properties of monolithic ceramics at room temperature, Part 5 Stat. Anal. (2006).
- [24] J.A. Krogstad, Y. Gao, J. Bai, J. Wang, D.M. Lipkin, C.G. Levi, In situ diffraction study of the high-temperature decomposition of t'-zirconia, *J. Am. Ceram. Soc.* 98 (2015) 247–254. <https://doi.org/10.1111/jace.13249>.

- 1  
2  
3  
4  
5  
6  
7  
8  
9  
10  
11  
12  
13  
14  
15  
16  
17  
18  
19  
20  
21  
22  
23  
24  
25  
26  
27  
28  
29  
30  
31  
32  
33  
34  
35  
36  
37  
38  
39  
40  
41  
42  
43  
44  
45  
46  
47  
48  
49  
50  
51  
52  
53  
54  
55  
56  
57  
58  
59  
60  
61  
62  
63  
64  
65
- [25] M. Yashima, M. Kakihana, M. Yoshimura, Metastable-stable phase diagrams in the zirconia-containing systems utilized in solid-oxide fuel cell application, *Solid State Ionics*. 86–88 (1996) 1131–1149. <http://www.sciencedirect.com/science/article/pii/0167273896003864> (accessed January 12, 2015).
- [26] J. Kondoh, Origin of the hump on the left shoulder of the X-ray diffraction peaks observed in Y<sub>2</sub>O<sub>3</sub>-fully and partially stabilized ZrO<sub>2</sub>, *J. Alloys Compd.* 375 (2004) 270–282. <https://doi.org/10.1016/j.jallcom.2003.11.129>.
- [27] M. Inokoshi, F. Zhang, K. Vanmeensel, J. De Munck, S. Minakuchi, I. Naert, J. Vleugels, B. Van Meerbeek, Residual compressive surface stress increases the bending strength of dental zirconia, *Dent. Mater.* 33 (2017) e147–e154. <https://doi.org/https://doi.org/10.1016/j.dental.2016.12.007>.
- [28] T. Kosmač, Č. Oblak, P. Jevnikar, N. Funduk, L. Marion, Strength and reliability of surface treated Y-TZP dental ceramics, *J. Biomed. Mater. Res.* 53 (2000) 304–313. [https://doi.org/10.1002/1097-4636\(2000\)53:4<304::AID-JBM4>3.0.CO;2-S](https://doi.org/10.1002/1097-4636(2000)53:4<304::AID-JBM4>3.0.CO;2-S).
- [29] T.A. Sulaiman, A.A. Abdulmajeed, K. Shahramian, L. Lassila, Effect of different treatments on the flexural strength of fully versus partially stabilized monolithic zirconia, *J. Prosthet. Dent.* 118 (2017) 216–220. <https://doi.org/https://doi.org/10.1016/j.prosdent.2016.10.031>.
- [30] X. Zhang, W. Liang, F. Jiang, Z. Wang, J. Zhao, C. Zhou, J. Wu, Effects of air-abrasion pressure on mechanical and bonding properties of translucent zirconia., *Clin. Oral Investig.* 25 (2021) 1979–88. <https://doi.org/10.1007/s00784-020-03506-y>.
- [31] S.S.M.P. Aung, T. Takagaki, S.K. Lyann, M. Ikeda, M. Inokoshi, A. Sadr, T. Nikaido, J. Tagami, Effects of alumina-blasting pressure on the bonding to super/ultra-translucent zirconia, *Dent. Mater.* 35 (2019) 730–739. <https://doi.org/10.1016/j.dental.2019.02.025>.
- [32] M. Wolfart, F. Lehmann, S. Wolfart, M. Kern, Durability of the resin bond strength to zirconia ceramic after using different surface conditioning methods., *Dent. Mater.* 23

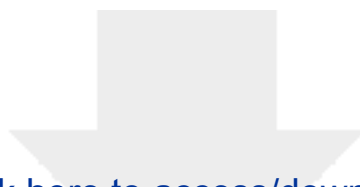
(2007) 45–50. <https://doi.org/10.1016/j.dental.2005.11.040>.

- 1 [33] M. Guazzato, L. Quach, M. Albakry, M. V Swain, Influence of surface and heat  
2 treatments on the flexural strength of Y-TZP dental ceramic, *J. Dent.* 33 (2005) 9–18.  
3 <https://doi.org/https://doi.org/10.1016/j.jdent.2004.07.001>.  
4  
5  
6  
7  
8 [34] A. Kocjan, A. Abram, A. Dakskobler, Impact strengthening of 3Y-TZP dental ceramic  
9 root posts, *J. Eur. Ceram. Soc.* 40 (2020) 4765–4773.  
10 <https://doi.org/10.1016/j.jeurceramsoc.2020.02.040>.  
11  
12  
13  
14  
15 [35] D. Baither, M. Bartsch, B. Baufeld, A. Tikhonovsky, A. Foitzik, M. Rühle, U.  
16 Messerschmidt, Ferroelastic and Plastic Deformation of t'-Zirconia Single Crystals, *J.*  
17 *Am. Ceram. Soc.* 84 (2004) 1755–1762. [https://doi.org/10.1111/j.1151-](https://doi.org/10.1111/j.1151-2916.2001.tb00911.x)  
18 [2916.2001.tb00911.x](https://doi.org/10.1111/j.1151-2916.2001.tb00911.x).  
19  
20  
21  
22  
23  
24  
25 [36] A. V Virkar, R.L. Matsumoto, Ferroelastic domain switching as a toughening mechanism  
26 in tetragonal zirconia, *J. Am. Ceram. Soc.* 69 (1986) C-224-C–226.  
27  
28  
29  
30 [37] M. Wendler, R. Belli, A. Petschelt, D. Mevec, W. Harrer, T. Lube, U. Lohbauer, R.  
31 Danzer, U. Lohbauer, Chairside CAD / CAM materials. Part 2: Flexural strength testing,  
32 *Dent. Mater.* 33 (2017) 99–109. <https://doi.org/10.1016/j.dental.2016.10.008>.  
33  
34  
35  
36  
37  
38  
39  
40  
41  
42  
43  
44  
45  
46  
47  
48  
49  
50  
51  
52  
53  
54  
55  
56  
57  
58  
59  
60  
61  
62  
63  
64  
65

**Declaration of interests**

The authors declare that they have no known competing financial interests or personal relationships that could have appeared to influence the work reported in this paper.

The authors declare the following financial interests/personal relationships which may be considered as potential competing interests:



[Click here to access/download](#)

**Supplementary Information**

Mirt et al\_Suppl Mater\_JECS\_2021.docx

